Article

Facile Lignin Extraction and Application as Natural UV Blockers in Cosmetic Formulations

Nguyen Van Duy *[ID], **Pavel Y. Tsygankov and Natalia V. Menshutina** [ID]

Department of Chemical and Pharmaceutical Engineering, Mendeleev University of Chemical Technology of Russia, 125480 Moscow, Russia; pavel.yur.tsygankov@gmail.com (P.Y.T.); chemcom@muctr.ru (N.V.M.)
* Correspondence: nguyenvanduylqd@gmail.com

Abstract: Natural compounds are becoming increasingly popular in the fields of pharmaceuticals and cosmetics. One such compound is lignin, a plant-derived aromatic polymer that serves as a natural anti-ultraviolet agent. Conventional methods for extracting lignin from plant materials typically involve performing procedures in harsh environments, such as dissolving it in highly alkaline solutions or subjecting it to treatment in acidic conditions. In this study, lignin was extracted from coconut husk under milder conditions, using neutral solvents and ultrasonic treatment, which allowed us to obtain lignin with significantly improved properties. The developed method facilitated the creation of light-colored lignin, which was employed as a natural ingredient in sunblock cream. Furthermore, for the sake of comparison, lignin was extracted under more rigorous conditions using the traditional method. The research findings confirm that the light-colored lignin sample exhibits a higher level of UV absorption. Furthermore, light-colored lignin demonstrates a synergistic effect when combined with commercial moisturizing creams and sunscreens, leading to a significant enhancement in their SPF performance against both UVA and direct sunlight exposure. This study highlights the potential value of incorporating lignin as a valuable natural ingredient in sunblock and cosmetic products.

Keywords: lignin; lignin color; UV absorption; sunscreen; cream

1. Introduction

The sunlight that reaches the Earth's surface encompasses ultraviolet (UVB, 290–320 nm and UVA, 320–400 nm), visible (VIS, 400–700 nm), and infrared (IR, 700–1000 nm) wavelengths [1]. Prolonged exposure to ultraviolet (UV) radiation can lead to various skin problems, such as sunburn, pigmentation spots, wrinkles, and skin cancer, which is the most common type of cancer [2,3]. Therefore, there is increasing interest in sunblock products, and clinical studies endorse the use of broad-spectrum (UVB + UVA) sunscreens to alleviate the damage linked to prolonged or frequent sun exposure. The efficacy of sunscreens in preventing UVB-induced sunburn is indicated by their sun protection factor (SPF). For instance, an individual using the recommended dose of SPF 20 sunscreen can stay in the sun without suffering sunburn 20 times longer than if not wearing sunscreen. Broad-spectrum sunscreens also effectively block a substantial portion of skin-aging UVA radiation. This involves ensuring that 10% of the protection provided by the sunscreen is for UVA, a characteristic measured by the UVA protection factor (UVA PF) [4]. Broad-spectrum chemical sunscreens are creams containing synthetic organic compounds that absorb both UVB and UVA rays [5]. In contrast, mineral-based (physical) sunscreens often feature nanoparticles of titanium dioxide (TiO_2) and/or zinc oxide (ZnO), which disperse and reflect UV rays [6,7]. However, the synthetic compounds used in chemical sunscreens not only pose risks to human health but also have adverse impacts on the environment. Additionally, it has been discovered that ZnO nanoparticles from physical sunscreens can harm coral reefs when released into the environment [8,9]. Therefore, there is currently

a trend in the cosmetic industry to replace synthetic sunscreen agents with natural and more cost-effective substances. Lignocellulosic biomass is the most abundant renewable natural resource on Earth, primarily composed of cellulose, hemicellulose, and lignin. Lignin, a heterogeneous and phenolic polymer, is present in most plants, constituting approximately 15 to 40% of the dry mass, and is the second most common renewable resource on Earth after cellulose [10]. Due to the presence of phenolic -OH groups, methoxy groups, carbonyl groups, and several other functional groups, lignin possesses excellent UV protection properties and has been incorporated into various materials for UV radiation protection [11,12]. Additionally, lignin and lignin-based products have been found to be non-cytotoxic and can be introduced into cells [13]. Lignin has been reported to significantly enhance the effectiveness of skin protection when added to sunscreen [14–17]. However, the dark color of lignin-based sunscreens presents a significant marketing challenge [18–20]. High temperatures and strongly alkaline pH values used in extraction processes typically lead to structural modifications of native lignin in lignocellulosic biomass, resulting in darkening [21–24].

In this study, ultrasonic extraction was employed to extract lignin from lignocellulosic (coconut husk) biomass under mild conditions: the mixture's temperature was maintained below 30 °C, and the pH value was kept neutral to prevent lignin color alteration. The resulting light-colored lignin was compared with dark lignin extracted using a mixture of ethanol and NaOH. Potential benefits of adding lignin to commercial creams for enhancing their sun protection properties were investigated. This research marked the first-time utilization of lignin extracted under gentle conditions using ultrasonic treatment as a component in sunblock cream.

2. Materials and Methods

2.1. Material

Sulfuric acid, 1,4-Dioxane, sodium hydroxide (NaOH), toluene, and ethanol were purchased from Merck (Darmstadt, Germany). The pure cream used was LOREN's soft moisturizer. The UV-filtering sunscreen used was LOREN SUN CARE protection with SPF 20 sun protection. Coconut husk was taken from fresh coconuts in Vietnam. The coconut husks were sun-dried, cut into 2 × 3 cm pieces, and then further dried at 105 °C for 4 h. Subsequently, the dried coconut coir pieces were crushed and sieved through a 0.1 mm mesh sieve to obtain the initial biomass.

2.2. Lignin Preparation

Lignin was extracted using the method described in [25]. The process diagram is depicted in Figure 1. Lignin yield was determined by comparing the dried lignin amount with the total lignin content in the coconut husk, which was approximately 30% by weight [26].

Method 1: Biomass was added to the solvent (95% ethanol) at a ratio of 1:20 (biomass weight to solvent volume). The mixture was stirred using a magnetic stirrer while heating to 80 °C for 4 h. Then, NaOH was added to the mixture in a 1:4 mass ratio to biomass, and the resulting mixture was stirred at 80 °C for 2 h. The mixture was then cooled to room temperature and filtered to collect the solution containing lignin. Sulfuric acid (pH 2) was added to this solution, causing lignin to precipitate. The obtained lignin was washed three times with water using a centrifuge to remove water-soluble impurities. Then, the resulting lignin was dried at 65 °C for 8 h (sample M1).

Method 2: Biomass was soaked in toluene at a ratio of 1:10 for four days, after which it was filtered. The precipitate was then added to 95% 1,4-dioxane at a ratio of biomass to 1,4-dioxane as 1:15. The mixture was placed in an ultrasonic bath (100 w), with the temperature maintained below 30 °C. The total ultrasonication time was 7 h, after which the mixture was allowed to stand for an additional two days. The mixture was then filtered to separate the precipitate from the filtrate using a Büchner funnel. The filtrate was evaporated in a rotary evaporator at 40 °C until it became viscous. To precipitate lignin, the obtained viscous liquid was added to distilled water in a 1:10 volume ratio. The resulting lignin was

washed three times with water using a centrifuge to remove water-soluble impurities. The lignin was dried using sublimation drying (sample M2).
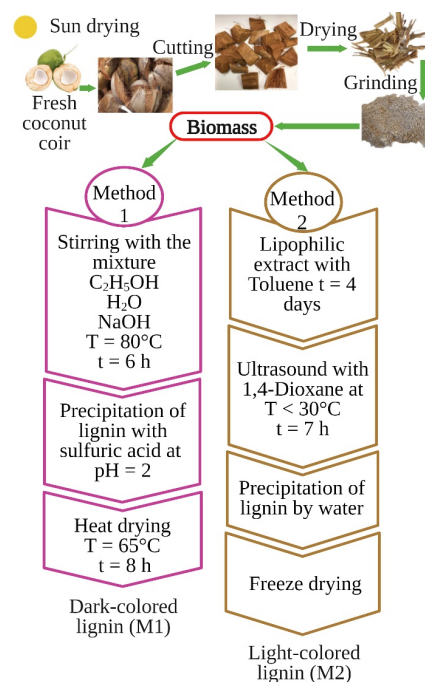

Figure 1. Process diagram for lignin extraction from coconut husk.

2.3. Characterization of Lignin

FT-IR spectra of lignin were acquired using a spectrophotometer (Prestige-21, Shimadzu, Kyoto, Japan) in the frequency range of 4000–500 cm^{-1}. About 1 mg of dried lignin sample was mixed well with 100 mg of dried KBr powder in an agate mortar. The mixture was finely ground and then compressed to form a tablet for FTIR analysis.

Proton ^{1}H NMR spectra were recorded for the extracted lignin using a Bruker Biospin AvanceNEO 600 MHz. The samples were dissolved in NaOD/D$_2$O solvent for NMR acquisition.

The UV-Vis method was used to determine the total phenolic hydroxyl (*phOH*) [27,28]. Lignin (1 mg/mL) was diluted in a mixture of dioxane and 0.2 M NaOH (1:1), and the solution was filtered through a 0.45 μm microfilter. The filtrate was further diluted in 0.2 M NaOH to obtain a concentration of 0.08 mg/mL. The UV spectrum was recorded in the range of 200–600 nm using a UNICO 2804 spectrophotometer, with lignin at pH 6 as the reference. The absorbance of the maximum spectra at 300 and 350 nm was used to calculate the total *phOH* using Equation (1):

$$phOH(\frac{mmol}{g}) = (0.425 \times A_{300nm}) + (0.812 \times A_{350nm}) \times \frac{1}{c \times a} \times \frac{10}{17} \tag{1}$$

where *A* is absorbance, *c* stands for lignin concentration, and *a* is path length (1 cm).

2.4. Preparation and UV Absorption Measurement of Creams with Added Lignin

Samples of lignin, M1 and M2, were added to a plain cream and a sunscreen cream, and then mixed on a magnetic stirrer at a speed of 500–600 rpm for 24 h. The entire mixing process was conducted at room temperature in the dark. After 24 h, it was observed that the lignin mixed well with the sunscreen cream, and no precipitation was observed, consistent with data from the literature [16].

The cream and sunscreen mixture with lignin was applied to a 3M Transpore Tape (4.5 cm^2) attached to the surface of a clean quartz cuvette (applied at 2 mg/cm^2). The samples were evenly spread over the surface and dried in the dark for 15 min [17]. UV

transmittance was measured using a UNICO 2804 spectrophotometer equipped with a holder for solid samples. Four points were scanned for each sample, and each scan was measured in the range from UVB (290–320 nm) to UVA (320–400 nm). After measuring UV light transmittance, the in vitro sun protection factor (SPF) was calculated using Equation (2) [16,17,29–31]:

$$SPF_{vitro} = \frac{\sum_{290nm}^{400nm} E_\lambda \times S_\lambda}{\sum_{290nm}^{400nm} E_\lambda \times S_\lambda \times 10^{-(A_\lambda \times C)}} \tag{2}$$

where S_λ is the ultraviolet irradiance, $W \cdot m^{-2} \cdot nm^{-1}$; λ is the wavelength of the source, A_λ is the optical absorption of the sample, and *C* is a constant coefficient for spectrum correction. The spectrum shape, reflecting the specific combination of UV filters in the tested product, remains constant [29]; E is the erythema action spectrum according to CIE (1999), calculated in relative units at each wavelength using the formulas [30]:

$$E = 1 \text{ for wavelengths } 250 \text{ nm} < \lambda \le 298 \text{ nm}, \tag{3}$$

$$E = 10^{0.094(298 - \lambda)} \text{ for wavelengths } 298 \text{ nm} < \lambda \le 328 \text{ nm}, \tag{4}$$

$$E = 10^{0.015(140 - \lambda)} \text{ for wavelengths } 328 \text{ nm} < \lambda \le 400 \text{ nm}. \tag{5}$$

The UVA protection factor (UVA PF) was calculated using Equation (6) [32]:

$$UVAPF = \frac{\sum_{320nm}^{400nm} E_\lambda \times I_\lambda \times \Delta\lambda}{\sum_{320nm}^{400nm} E_\lambda \times I_\lambda \times 10^{-A_\lambda} \times \Delta\lambda} \tag{6}$$

If $\Delta\lambda$ is sufficiently small, the equation for the *UVA* protection factor can be simplified. In this case, where I_λ represents the biological action spectrum for UVA, both E_λ and I_λ are equal to one for all *UVA* wavelengths, as proposed by Ferrero et al. [32].

2.5. UV Irradiation Effects

Sunscreens, with and without the addition of lignin, were exposed to UV light to investigate the effects of UV irradiation. The samples were prepared in the same way as for SPF measurement, by applying them to a quartz plate and then irradiating them with UV. Following exposure to UV radiation, transmittance was measured in the range from 290 nm to 400 nm.

2.6. Solar Radiation Effects

The creams, with and without the addition of lignin, were exposed to direct sunlight (at 12 noon, with a temperature of 21 degrees Celsius and a clear sky) to investigate their performance under real sun exposure. The samples were prepared in the same manner as for the SPF measurement by placing them on a quartz plate and then exposing them to sunlight. UV transmittance was measured from 290 nm to 400 nm during the exposure.

3. Results and Discussion

3.1. Characteristics of the Obtained Lignin Samples

In this study, the yields of lignin M1 and lignin M2 extracted from coir were determined to be 34% and 19%, respectively, based on the weight of the biomass. The color of lignin samples M1 and M2 extracted from coir were visually compared. As depicted in Figure 2, M1 appeared as dark brown while M2 appeared as pale yellow.

(**a**)   (**b**)

Figure 2. Images of the obtained samples M1 (**a**) and M2 (**b**).

The dark brown color of lignin M1 is probably due to the formation of condensation, decomposition and oxidation products during separation under high temperature and pH conditions. Using Equation (1), the contents of phenolic OH groups in samples M1 and M2 were determined, and the results in Table 1 show that M1 had a total content of phenolic OH groups of 2.82 mmol/g, while for M2, it was 3.15 mmol/g. M2 exhibited a higher phenolic OH group content than M1, likely due to the cleavage of β-O-4 bonds and/or condensation reactions of lignin. This process augments the phenolic hydroxyl group content, leading to increased active sites on the side chain and the formation of more conjugated structures [33–35].

Table 1. Phenolic hydroxyl group content (*phOH*).

Sample	Total *phOH* (mmol/g)
M1	2.82 ± 0.22
M2	3.15 ± 0.10

FT-IR spectra, depicted in Figure 3, were acquired for samples M1 and M2. The IR spectra exhibited a broad peak at 3400 cm^{-1}, indicating the stretching vibration of phenolic and aliphatic hydroxyl groups present in the lignin samples. Two adjacent signals at 2935 cm^{-1} and 2847 cm^{-1} were attributed to the stretching vibrations of C-H bonds in the -CH$_2$ and -CH$_3$ groups [36]. The peak at 1710 cm^{-1}, which corresponds to C=O stretching in α, β-unsaturated aldehydes, unconjugated ketones, or esters, is not clearly observed in the spectrum of lignin M1 as it is in the spectrum of lignin M2. This is presumably due to the harsher conditions in obtaining the M1 sample and the bond cleavage. Additionally, there is a broad peak at 1650 cm^{-1}, indicating the stretching of C=O in p-substituted conjugated aryl ketone, which can be attributed to the formation of quinoid structures responsible for the darker color of lignin M1 [19,36,37]. The absorption peaks of aromatic skeleton vibrations at 1601 cm^{-1} and 1510 cm^{-1} may be enhanced by the cleavage of β-O-4 bonds and/or condensation reactions. These processes can lead to an increase in the number of phenolic OH groups (auxochromes) and/or the formation of conjugated structures, such as coniferaldehyde (chromophores). A deformation of the peak at 1451 cm^{-1}, related to C-H and methoxy groups, is observed. The peak at 1423 cm^{-1} was only detected in the spectrum of lignin M1, indicating the formation of new conjugated double bonds during the lignin separation process [17,21,38]. The stretching of G and S rings is observed at 1370 cm^{-1}. The vibration of the benzene ring of S units is detected at 1325 cm^{-1}, and for G units, it occurs at 1271 cm^{-1} and 1218 cm^{-1} [37,39]. Additionally, the peak at 1160 cm^{-1} corresponds to conjugated C=O in the ether of lignin of the H-G-S type, but in both spectra of M1 and M2, the signal is too weak, indicating that the lignin fraction studied in this work is primarily of the G-S type. The peak observed at 1121 cm^{-1} indicates the presence of a syringyl group in lignin, as it represents the stretching of the C-H structure of S [36].
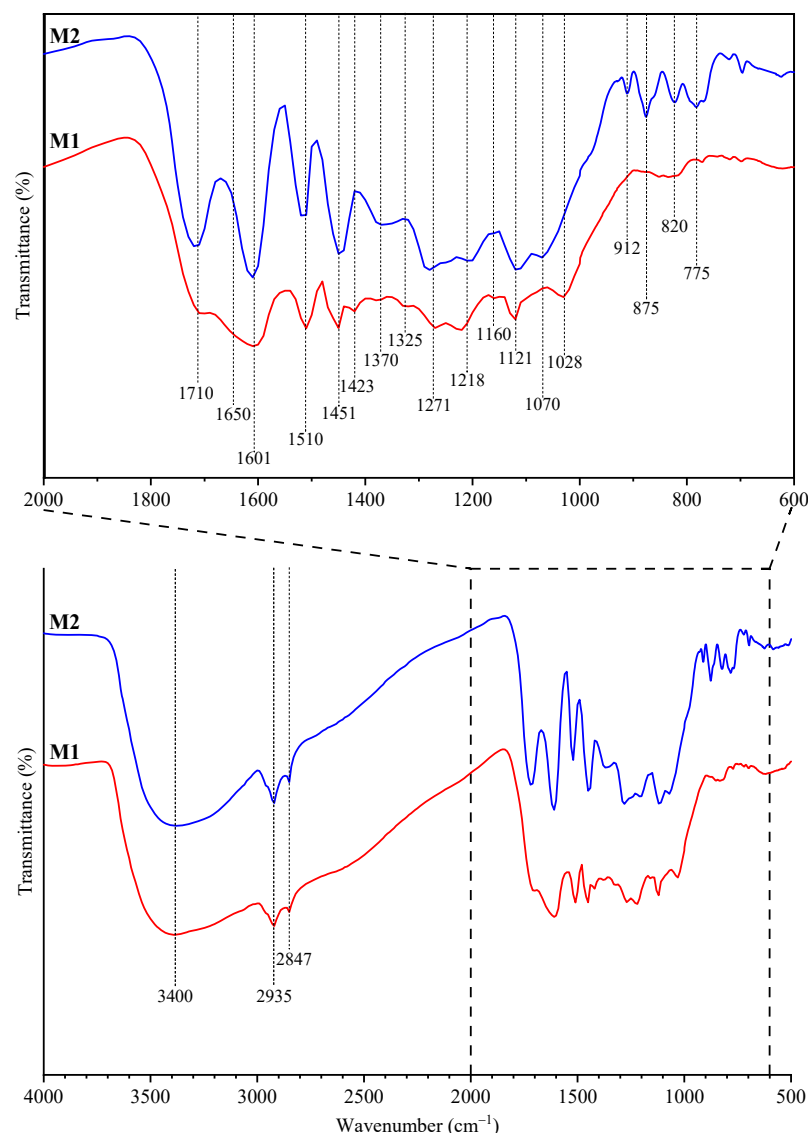
Figure 3. FTIR spectra of extracted lignin.

The signal observed at 1070 cm^{-1} in the spectrum of lignin M2 is characteristic of the stretching of C-O in secondary alcohols and fatty ethers. These functional groups are preserved due to the less harsh conditions used for extracting lignin from sample M2 compared to lignin M1. On the other hand, the spectrum of lignin M1 only shows the signal of G units at 1028 cm^{-1} [39,40]. Peaks at 912 cm^{-1}, 875 cm^{-1}, 820 cm^{-1}, and 775 cm^{-1} in the lignin M2 spectrum indicate the presence of G rings [36–40], suggesting a higher content of aromatic rings (specifically G rings) in lignin M2 compared to M1. Moreover, commercial sunscreens often contain aromatic compounds as active ingredients (e.g., octocrylene, ethylhexyl salicylate, butyl methoxydibenzoylmethane, and ethylhexyl triazone) [17]. Therefore, lignin extracted from biomass with a higher content of aromatic rings may provide better protection against UV radiation.

The chemical structure of the extracted lignin and the associated functional groups were further characterized using ^{1}H NMR spectroscopy, as shown in Figure 4. The peaks between 0.8 and 2.0 ppm corresponded to the aliphatic hydrocarbon region, mainly consisting of primary, secondary, and tertiary alkyl groups [41–43]. The peaks between 1.4 and 2.2 ppm correspond to the proton of aliphatic acetates, while the signals at 2.2 to 2.5 ppm represent the proton of aromatic acetates [43,44].
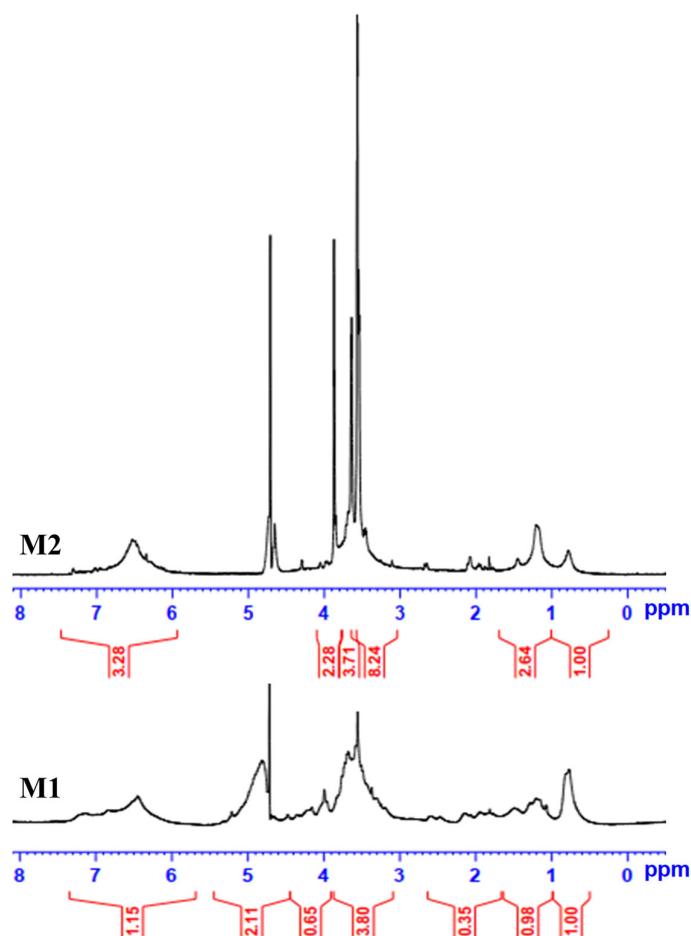
Figure 4. ^{1}H NMR spectra of extracted lignin.

The proton signals of the methoxy group, which are associated with the G and S unit ratio, are observed in the peaks between 3.1 and 4.0 ppm [42,45]. The resonance signal around 4.2 to 4.5 ppm is due to the presence of hydrogen within the -HC-O-CH$_2$- group, which is connected through an ether linkage [46]. The signal around 5 ppm could be a trace of water (in D$_2$O solvent and/or in the sample). The peaks corresponding to the presence of aromatic protons in lignin appear between 6.5 and 8.5 ppm. The signals corresponding to the aromatic protons in the syringyl (S) propane appear between 6.1 and 6.7 ppm [47,48]. The spectral resonance signals observed in the 6.5 to 7.5 ppm range could be attributed to the aromatic protons, encompassing guaiacyl, syringyl, and p-hydroxyphenyl components [49]. Overall, most of the functional groups corresponding to the lignin structure were preserved and present in the extracted lignin, indicating that the lignin extraction process did not significantly alter the native structure of the lignin, preserving the majority of functional groups. The M2 and M1 spectra demonstrate almost similar peaks, but the intensity of the signals is higher for the M2 sample spectra. The integrated intensity of a signal in a ^{1}H NMR spectrum provides a ratio for the number of hydrogens contributing to the signal. This indicates that although both lignin samples have similar functional groups, M2 lignin has a higher number of functional groups than M1 lignin. Consequently, this result signifies the higher total phenolic content of the M2 lignin sample [50].

3.2. Ultraviolet Absorption Potential of Lignin

To investigate the absorbance capacity in the range of 200 nm to 600 nm, solutions of samples M1 and M2 were prepared in 0.1 M NaOH. Figure 5 displays the UV absorption spectra, with both types of lignin exhibiting prominent peaks: M1 in the range of 200 nm to 230 nm, associated with non-conjugated phenolic groups (π-π*), and M2 in the range of 280

to 303 nm, attributed to conjugated phenolic groups (n-π*) [51,52]. The presence of aromatic rings, methoxy groups, and conjugated double bonds in lignin contributes to its ultraviolet absorption [53]. However, M2 exhibits a broader and stronger absorption across the entire ultraviolet region (280–400 nm) compared to the M1 sample. M2 shows higher absorption both in the ultraviolet A range (320–400 nm) and the ultraviolet B range (280–320 nm), indicating more effective ultraviolet screening. This is attributed to the higher content of phenolic groups (-OH), methoxy, carbonyl, and other functional groups [15,53,54].
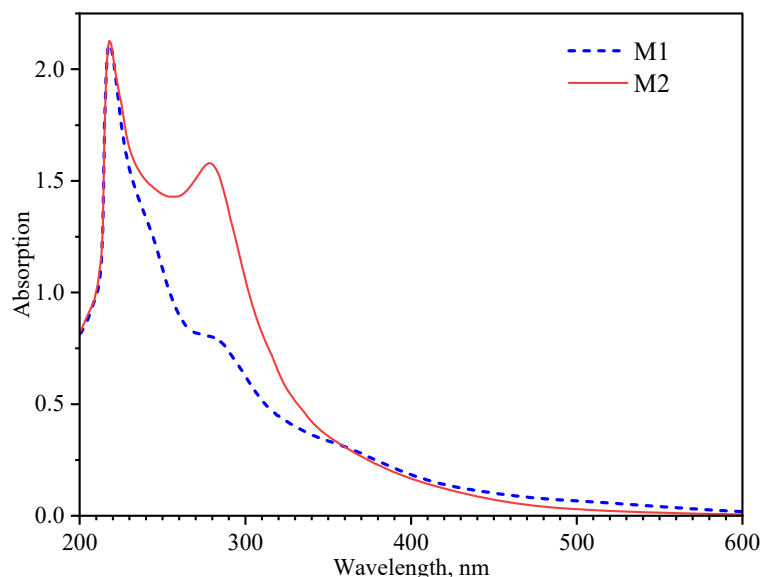

Figure 5. UV-absorption activity of the isolated lignin.

3.3. Assessing the UV Protection of Lignin in Combination with a Commercial Moisturizing Cream

The effectiveness of lignin samples as ultraviolet protection agents was assessed by blending them with a commercial moisturizing cream (LOREN) and evaluating their sun protection factor (SPF). Table 2 presents the SPF values for creams containing different concentrations (1 wt.%, 5 wt.%, and 10 wt.%) of lignin samples M1 and M2. The LOREN cream exhibited minimal UV absorption in both the UVA and UVB ranges, with an SPF value of approximately 1.1. However, the addition of lignin samples to the cream resulted in a proportional increase in SPF values. Notably, the SPF value increased to 10.7 with the concentration of lignin M2 at 10 wt.%.

Table 2. SPF of the moisturizing cream blended with lignin.

SPF Value	Lignin	0% Lignin (wt.%)	1% Lignin (wt.%)	5% Lignin (wt.%)	10% Lignin (wt.%)
SPF of cream with lignin M1		1.1 ± 0.1 [1]	1.9 ± 0.1	3.7 ± 0.1	8.7 ± 0.3
SPF of cream with lignin M2			2.4 ± 0.1	7.6 ± 0.2	10.7 ± 0.4

[1] The SPF value of the cream without lignin addition.

It is worth mentioning that lignin sample M2 demonstrated stronger ultraviolet absorption compared to lignin sample M1. Consequently, lignin sample M2 holds greater promise as a natural ingredient in sunscreen formulations.

Further investigations were carried out on cream–lignin sample mixtures under UV radiation (7.5 mW/cm^2) and direct sunlight at noon. The SPF indices were measured over a specified period, and the results are presented in Figures 6 and 7. The obtained results indicate that the addition of lignin to a regular moisturizing cream enhances its SPF. While the samples with 1% M1 and 1% M2 did not show significant changes in SPF when exposed

to UV rays, increasing the concentration of lignin resulted in higher SPF values, especially after 20 min of UV exposure.
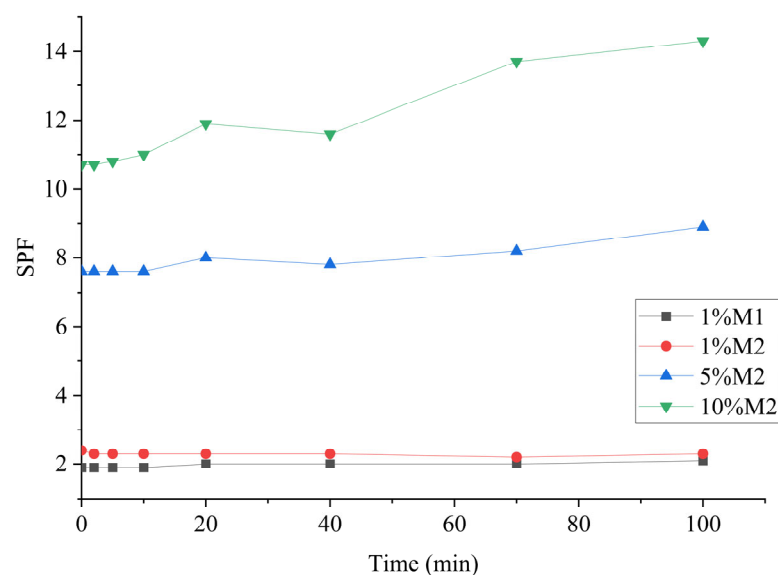

Figure 6. The impact of UV radiation on the SPF of the moisturizing cream blended with lignin.
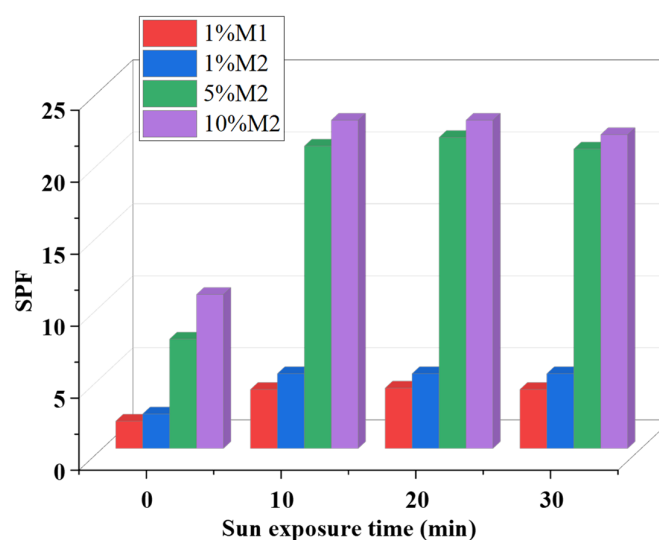

Figure 7. Effect of direct sunlight on the SPF of the moisturizing cream mixed with lignin.

The hydroxyl groups play a key role in higher SPF values, as demonstrated in Figure 6. The increase in SPF over time of UV exposure can be attributed to the chemical interaction between lignin hydroxyl groups and the moisturizing cream under UV radiation [15].

For the cream samples with lignin exposed to direct sunlight, the SPF value significantly increased after 10 min but remained nearly constant during the following 30 min of exposure. These results confirm that lignin is a natural polymer with excellent UV resistance, and lignin M2 is an effective component for sun protection. Lignin incorporated into the sunscreen absorbs UV radiation, as shown in Figure 8. Sunscreen containing lignin functions as a UV filter, as their mode of action involves absorbing UV radiation, which results from several chemical changes in lignin molecules. When lignin is exposed to UV radiation, part of the incident energy is released as heat, while the remaining energy causes the phenolic hydroxyl groups of lignin to first form phenoxyl radicals, which later become quinonoid structures [15,19,55]. Combining lignin with other organic UV filters present in commercial sunscreens is an effective way to enhance protection against a broad spectrum

of UV radiation (UVA and UVB) and increase the SPF (sun protection factor), thus creating a new, more efficient sun protection product.
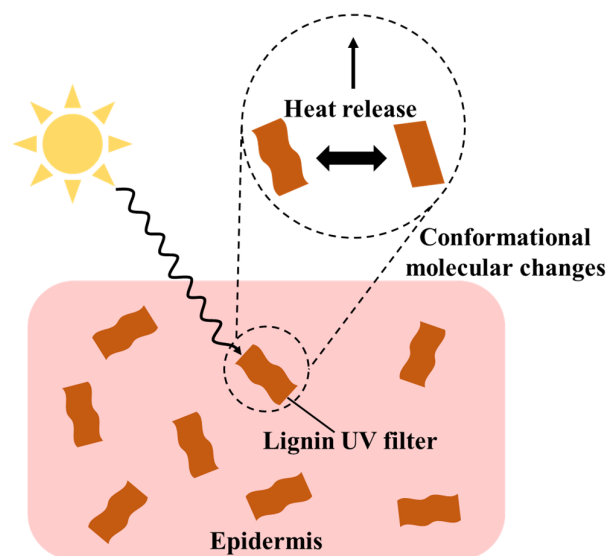

Figure 8. Mode of action of lignin UV filters on the epidermis [15,55].

3.4. Mixture Effects of Lignin with Commercial Sunscreen

Samples of lignin M1 and M2 were blended with a commercial sunscreen cream (LOREN SPF 20). The efficacy of UV radiation blocking was assessed, and the results are presented in Table 3. Introducing M1 or M2 at a concentration of 4% by mass into the sunscreen cream led to nearly a twofold increase in SPF and UVA-PF values. It is considered that lignin is compatible with organic sunscreen agents, and the UV protection of lignin is provided by its aromatic rings and functional groups. The observed synergistic effect in mixed sunscreens with lignin can be explained by non-covalent π-interactions between the π-bonds of the aromatic rings present in lignin and the active chemical components of sunscreens.

Table 3. Sunscreen protection factor (SPF) and ultraviolet A protection factor (UVA PF) of sunscreen cream with lignin additives.

Lignin (wt.%)	M1		M2	
	SPF (290–400 nm)	**UVA PF** (320–400 nm)	**SPF** (290–400 nm)	**UVA PF** (320–400 nm)
0%	20.0 ± 0.3 [2]	3.2 ± 0.1 [3]		
1%	24.6 ± 0.4	3.8 ± 0.1	27.3 ± 0.5	4.0 ± 0.2
2%	26.7 ± 0.3	4.9 ± 0.2	30.2 ± 0.2	5.4 ± 0.2
3%	29.8 ± 0.6	5.6 ± 0.1	34.4 ± 0.5	6.2 ± 0.1
4%	32.7 ± 0.7	7.8 ± 0.2	36.1 ± 0.8	8.9 ± 0.3

[2] The value of SPF for the sunscreen cream without the addition of lignin. [3] The value of UVA PF for sunscreen cream without the addition of lignin.

Furthermore, the effect of adding lignin to the sunscreen cream on its ability to block UV radiation over time was investigated. Samples of sunscreen cream with and without lignin were exposed to UV radiation (7.5 mW/cm^2) for a specific duration, and SPF values were determined. Figure 9 shows that the SPF value of the sunscreen cream without lignin decreased after 5 min of exposure, but after 20 min of exposure, the SPF value remained almost unchanged. In contrast, the samples of sunscreen cream with added lignin showed an increase in SPF value after 20 min of UV exposure, and the SPF value reached its maximum between 60 to 80 min. This increase in SPF was proportional to the

concentration of lignin in the original sunscreen cream. This can be explained by the fact that UV irradiation could cause lignin to react with some active ingredients of sunscreen, forming conjugated color groups more efficiently [14,15].
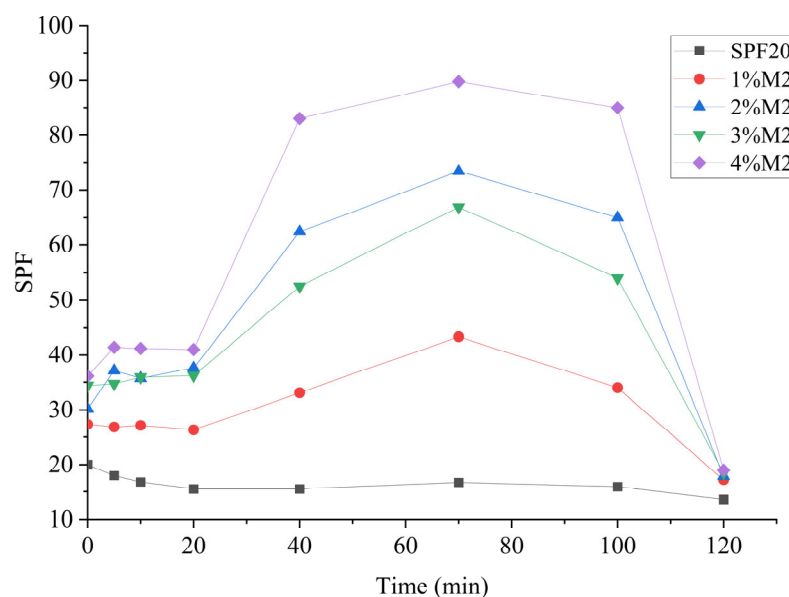

Figure 9. Effects of UV rays on sunscreens with and without lignin.

A comparison of sunscreen without lignin and with the addition of 1% by weight of M1 and M2 is presented in Figure 10.
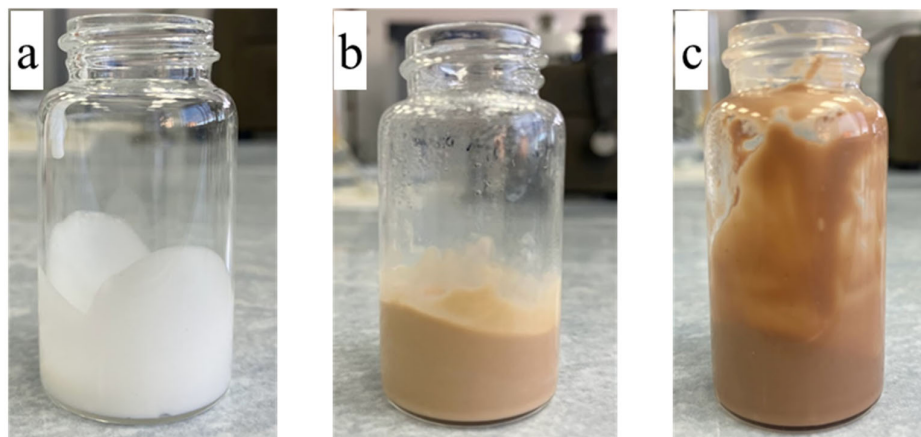

Figure 10. Photographs of the sunscreen without lignin (**a**) and with the addition of 1% by weight of lignin M2 (**b**) and M1 (**c**).

The results showed that the sunscreen with the addition of lignin M2 resulted in a more appealing cream color. Additionally, sunscreens mixed with lignin M2 demonstrated better UV absorption.

4. Conclusions

In this study, lignin obtained from coconut husk using the ultrasound method under mild conditions was used for the first time as a natural protective agent against ultraviolet radiation. The obtained lignin samples (M1 and M2) demonstrated high protection against ultraviolet radiation and sunlight, especially when mixed with commercial cream. In comparison to M1, which was obtained under harsh conditions (dissolution in alkaline environments at pH 14 and subsequent treatment in acidic pH 2, at temperatures exceeding

80 °C), M2 had a lighter color. M2 also demonstrated a synergistic effect with commercial sunscreens, as the SPF of products containing M2 increased from 20.0 to 36.1 after exposure to UV radiation and direct sunlight. The study demonstrates that lignin M2 has great potential as a natural ingredient in sunscreens and cosmetics.

Author Contributions: Conceptualization, N.V.M., P.Y.T. and N.V.D.; methodology, N.V.D.; investigation, N.V.D.; writing—original draft preparation, N.V.D.; writing—review and editing, N.V.M. and P.Y.T.; supervision, P.Y.T.; project administration, N.V.M. All authors have read and agreed to the published version of the manuscript.

Data Availability Statement: Data will be made available on request.

Conflicts of Interest: The authors declare that they have no known competing financial interests or personal relationships that could have appeared to influence the work reported in this paper.

References

1. Hudson, L.; Rashdan, E.; Bonn, C.A.; Chavan, B.; Rawlings, D.; Birch-Machin, M.A. Individual and combined effects of the infrared, visible, and ultraviolet light components of solar radiation on damage biomarkers in human skin cells. *FASEB J.* **2020**, *34*, 3874–3883. [CrossRef]
2. Hirst, N.G.; Gordon, L.G.; Scuffham, P.A.; Green, A.C. Lifetime cost-effectiveness of skin cancer prevention through promotion of daily sunscreen use. *Value Health* **2012**, *15*, 261–268. [CrossRef] [PubMed]
3. Lyons, A.B.; Trullas, C.; Kohli, I.; Hamzavi, I.H.; Lim, H.W. Photoprotection beyond ultraviolet radiation: A review of tinted sunscreens. *J. Am. Acad. Dermatol.* **2021**, *84*, 1393–1397. [CrossRef] [PubMed]
4. Diaz, J.H.; Nesbitt, L.T., Jr. Sun exposure behavior and protection: Recommendations for travelers. *J. Travel Med.* **2013**, *20*, 108–118. [CrossRef] [PubMed]
5. Beisl, S.; Friedl, A.; Miltner, A. Lignin from Micro- to Nanosize: Applications. *Int. J. Mol. Sci.* **2017**, *18*, 2367. [CrossRef] [PubMed]
6. Gause, S.; Chauhan, A. UV-blocking potential of oils and juices. *Int. J. Cosmet. Sci.* **2016**, *38*, 354–363. [CrossRef]
7. Rabinovich, L.; Kazlouskaya, V. Herbal sun protection agents: Human studies. *Clin. Dermatol.* **2018**, *36*, 369–375. [CrossRef]
8. Butt, S.T.; Christensen, T. Toxicity and Phototoxicity of Chemical Sun Filters. *Radiat. Prot. Dosim.* **2000**, *91*, 283–286. [CrossRef]
9. Corinaldesi, C.; Marcellini, F.; Nepote, E.; Damiani, E.; Danovaro, R. Impact of inorganic UV filters contained in sunscreen products on tropical stony corals (*Acropora* spp.). *Sci. Total Environ.* **2018**, *637–638*, 1279–1285. [CrossRef]
10. Norgren, M.; Edlund, H. Lignin: Recent advances and emerging applications. *Curr. Opin. Colloid Interface Sci.* **2014**, *19*, 409–416. [CrossRef]
11. Shankar, S.; Rhim, J.W.; Won, K. Preparation of poly(lactide)/lignin/silver nanoparticles composite films with UV light barrier and antibacterial properties. *Int. J. Biol. Macromol.* **2018**, *107*, 1724–1731. [CrossRef] [PubMed]
12. Guo, Y.; Tian, D.; Shen, F.; Yang, G.; Long, L.; He, J.; Song, C.; Zhang, J.; Zhu, Y.; Huang, C.; et al. Transparent Cellulose/Technical Lignin Composite Films for Advanced Packaging. *Polymers* **2019**, *11*, 1455. [CrossRef] [PubMed]
13. Tortora, M.; Cavalieri, F.; Mosesso, P.; Ciaffardini, F.; Melone, F.; Crestini, C. Ultrasound driven assembly of lignin into microcapsules for storage and delivery of hydrophobic molecules. *Biomacromolecules* **2014**, *15*, 1634–1643. [CrossRef] [PubMed]
14. Qian, Y.; Qiu, X.; Zhu, S. Lignin: A nature-inspired sun blocker for broad-spectrum sunscreens. *Green Chem.* **2015**, *17*, 320–324. [CrossRef]
15. Qian, Y.; Qiu, X.; Zhu, S. Sunscreen Performance of Lignin from Different Technical Resources and Their General Synergistic Effect with Synthetic Sunscreens. *ACS Sustain. Chem. Eng.* **2016**, *4*, 4029–4035. [CrossRef]
16. Lee, S.C.; Tran, T.M.T.; Choi, J.W.; Won, K. Lignin for white natural sunscreens. *Int. J. Biol. Macromol.* **2019**, *122*, 549–554. [CrossRef] [PubMed]
17. Lee, S.C.; Yoo, E.; Lee, S.H.; Won, K. Preparation and Application of Light-Colored Lignin Nanoparticles for Broad-Spectrum Sunscreens. *Polymers* **2020**, *12*, 699. [CrossRef] [PubMed]
18. Kai, D.; Tan, M.J.; Chee, P.L.; Chua, Y.K.; Yap, Y.L.; Loh, X.J. Towards lignin-based functional materials in a sustainable world. *Green Chem.* **2016**, *18*, 1175–1200. [CrossRef]
19. Wang, J.; Deng, Y.; Qian, Y.; Qiu, X.; Ren, Y.; Yang, D. Reduction of lignin color via one-step UV irradiation. *Green Chem.* **2016**, *18*, 695–699. [CrossRef]
20. Tran, M.H.; Phan, D.-P.; Lee, E.Y. Review on lignin modifications toward natural UV protection ingredient for lignin-based sunscreens. *Green Chem.* **2021**, *23*, 4633–4646. [CrossRef]

21. Yao, C.; Yongming, F.; Jianmin, G.; Houkun, L. Coloring characteristics of in situ lignin during heat treatment. *Wood Sci. Technol.* **2010**, *46*, 33–40. [CrossRef]

22. Qiu, X.; Yu, J.; Yang, D.; Wang, J.; Mo, W.; Qian, Y. Whitening Sulfonated Alkali Lignin via H2O2/UV Radiation and Its Application As Dye Dispersant. *ACS Sustain. Chem. Eng.* **2017**, *6*, 1055–1060. [CrossRef]

23. Zhang, H.; Bai, Y.; Yu, B.; Liu, X.; Chen, F. A practicable process for lignin color reduction: Fractionation of lignin using methanol/water as a solvent. *Green Chem.* **2017**, *19*, 5152–5162. [CrossRef]

24. Zhang, H.; Bai, Y.; Zhou, W.; Chen, F. Color reduction of sulfonated eucalyptus kraft lignin. *Int. J. Biol. Macromol.* **2017**, *97*, 201–208. [CrossRef]

25. Duy, N.V.; Tsygankov, P.Y.; Menshutina, N.V. Hybrid Aerogels Based on Lignin, Derived from Vegetable Raw Materials. *ChemChemTech* **2023**, *66*, 75–83. [CrossRef]

26. Reddy, N. *Sustainable Applications of Coir and Other Coconut By-Products*; Springer International Publishing: Cham, Switzerland, 2019; p. 63. [CrossRef]

27. Serrano, L.; Esakkimuthu, E.S.; Marlin, N.; Brochier-Salon, M.-C.; Mortha, G.; Bertaud, F. Fast, Easy, and Economical Quantification of Lignin Phenolic Hydroxyl Groups: Comparison with Classical Techniques. *Energy Fuels* **2018**, *32*, 5969–5977. [CrossRef]

28. Solihat, N.N.; Santoso, E.B.; Karimah, A.; Madyaratri, E.W.; Sari, F.P.; Falah, F.; Iswanto, A.H.; Ismayati, M.; Lubis, M.A.R.; Fatriasari, W.; et al. Physical and Chemical Properties of *Acacia mangium* Lignin Isolated from Pulp Mill Byproduct for Potential Application in Wood Composites. *Polymers* **2022**, *14*, 491. [CrossRef] [PubMed]

29. Wendel, V.; Uhlmann, B.; Mann, T.; Klette, E. In Vitro Test Method to Assess the UVA Protection Performance of Sun Care Products. European Patent EP1291640A1, 12 March 2003.

30. *ISO 24444:2019*; Cosmetics Sun Protection Test Methods In Vivo Determination of the Sun Protection Factor (SPF). International Organization for Standardization: Geneva, Switzerland, 2019.

31. Gers-Barlag, H.; Klette, E.; Bimczok, R.; Springob, C.; Finkel, P.; Rudolph, T.; Gonzenbach, H.U.; Schneider, P.H.; Kockott, D.; Heinrich, U.; et al. In vitro testing to assess the UVA protection performance of sun care products. *Int. J. Cosmet. Sci.* **2001**, *23*, 3–14. [CrossRef]

32. Ferrero, L.; Pissavini, M.; Marguerie, S.; Zastrow, L. Sunscreen in vitro spectroscopy: Application to UVA protection assessment and correlation with in vivo persistent pigment darkening. *Int. J. Cosmet. Sci.* **2002**, *24*, 63–70. [CrossRef]

33. Constant, S.; Wienk, H.L.J.; Frissen, A.E.; Peinder, P.d.; Boelens, R.; van Es, D.S.; Grisel, R.J.H.; Weckhuysen, B.M.; Huijgen, W.J.J.; Gosselink, R.J.A.; et al. New insights into the structure and composition of technical lignins: A comparative characterisation study. *Green Chem.* **2016**, *18*, 2651–2665. [CrossRef]

34. Zhang, Y.; Yang, L.; Wang, D.; Li, D. Structure elucidation and properties of different lignins isolated from acorn shell of Quercus variabilis Bl. *Int. J. Biol. Macromol.* **2018**, *107*, 1193–1202. [CrossRef] [PubMed]

35. Farid, T.; Wang, Y.; Rafiq, M.I.; Ali, A.; Tang, W. Porous flexible wood scaffolds designed for high-performance electrochemical energy storage. *ACS Sustain. Chem. Eng.* **2022**, *10*, 7078–7090. [CrossRef]

36. Song, Y.; Ji, H.; Shi, X.; Yang, X.; Zhang, X. Successive organic solvent fractionation and structural characterization of lignin extracted from hybrid poplar by deep eutectic solvent for improving the homogeneity and isolating narrow fractions. *Renew. Energy* **2020**, *157*, 1025–1034. [CrossRef]

37. Su, X.; Fu, Y.; Shao, Z.; Qin, M.; Li, X.; Zhang, F. Light-colored lignin isolated from poplar by ultrasound-assisted ethanol extraction: Structural features and anti-ultraviolet and anti-oxidation activities. *Ind. Crops Prod.* **2022**, *176*, 114359. [CrossRef]

38. Singh, S.K.; Dhepe, P.L. Isolation of lignin by organosolv process from different varieties of rice husk: Understanding their physical and chemical properties. *Bioresour. Technol.* **2016**, *221*, 310–317. [CrossRef] [PubMed]

39. Bock, P.; Nousiainen, P.; Elder, T.; Blaukopf, M.; Amer, H.; Zirbs, R.; Potthast, A.; Gierlinger, N. Infrared and Raman spectra of lignin substructures: Dibenzodioxocin. *J. Raman Spectrosc.* **2020**, *51*, 422–431. [CrossRef] [PubMed]

40. Melro, E.; Filipe, A.; Sousa, D.; Medronho, B.; Romano, A. Revisiting lignin: A tour through its structural features, characterization methods and applications. *New J. Chem.* **2021**, *45*, 6986–7013. [CrossRef]

41. Deepa, A.K.; Dhepe, P.L. Lignin depolymerization into aromatic monomers over solid acid catalysts. *ACS Catal.* **2015**, *5*, 365–379. [CrossRef]

42. Li, L.; Wu, Z.; Xi, X.; Liu, B.; Cao, Y.; Xu, H.; Hu, Y. A bifunctional brønsted acidic deep eutectic solvent to dissolve and catalyze the depolymerization of alkali lignin. *J. Renew. Mater.* **2021**, *9*, 219–235. [CrossRef]

43. Rashid, T.; Kait, C.F.; Regupathi, I.; Murugesan, T. Dissolution of kraft lignin using Protic Ionic Liquids and characterization. *Ind. Crops Prod.* **2016**, *84*, 284–293. [CrossRef]

44. Abd Latif, N.H.; Brosse, N.; Ziegler-Devin, I.; Chrusiel, L.; Hashim, R.; Hussin, M.H. Structural characterization of modified coconut husk lignin via steam explosion pretreatment as a renewable phenol substitutes. *Int. J. Biol. Macromol.* **2023**, *253*, 127210. [CrossRef]

45. Cassales, A.; Ramos, L.A.; Frollini, E. Synthesis of bio-based polyurethanes from Kraft lignin and castor oil with simultaneous film formation. *Int. J. Biol. Macromol.* **2020**, *145*, 28–41. [CrossRef]

46. Kim, D.; Cheon, J.; Kim, J.; Hwang, D.; Hong, I.; Kwon, O.H.; Park, W.H.; Cho, D. Extraction and characterization of lignin from black liquor and preparation of biomass-based activated carbon there-from. *Carbon Lett.* **2017**, *22*, 81–88. [CrossRef]

47. Mankar, A.R.; Pandey, A.; Pant, K. Microwave-assisted extraction of lignin from coconut coir using deep eutectic solvents and its valorization to aromatics. *Bioresour. Technol.* **2022**, *345*, 126528. [CrossRef] [PubMed]

48. Oruganti, R.K.; Sunar, S.L.; Panda, T.K.; Shee, D.; Bhattacharyya, D. Kraft lignin recovery from de-oiled Jatropha curcas seed by potassium hydroxide pretreatment and optimization using response surface methodology. *Bioresour. Technol. Rep.* **2023**, *23*, 101572. [CrossRef]

49. Nivedha, M.; Manisha, M.; Gopinath, M.; Baskar, G.; Tamilarasan, K. Fractionation, characterization, and economic evaluation of alkali lignin from saw industry waste. *Bioresour. Technol.* **2021**, *335*, 125260. [CrossRef]

50. Dhara, S.; Samanta, N.S.; Uppaluri, R.; Purkait, M. High-purity alkaline lignin extraction from Saccharum ravannae and optimization of lignin recovery through response surface methodology. *Int. J. Biol. Macromol.* **2023**, *234*, 123594. [CrossRef] [PubMed]

51. Alzagameem, A.; Khaldi-Hansen, B.E.; Buchner, D.; Larkins, M.; Kamm, B.; Witzleben, S.; Schulze, M. Lignocellulosic Biomass as Source for Lignin-Based Environmentally Benign Antioxidants. *Molecules* **2018**, *23*, 2664. [CrossRef]

52. Rumpf, J.; Do, X.T.; Burger, R.; Monakhova, Y.B.; Schulze, M. Extraction of High-Purity Lignins via Catalyst-free Organosolv Pulping from Low-Input Crops. *Biomacromolecules* **2020**, *21*, 1929–1942. [CrossRef]

53. Zhang, Y.; Naebe, M. Lignin: A Review on Structure, Properties, and Applications as a Light-Colored UV Absorber. *ACS Sustain. Chem. Eng.* **2021**, *9*, 1427–1442. [CrossRef]

54. Zhang, H.; Liu, X.; Fu, S.; Chen, Y. Fabrication of Light-Colored Lignin Microspheres for Developing Natural Sunscreens with Favorable UV Absorbability and Staining Resistance. *Ind. Eng. Chem. Res.* **2019**, *58*, 13858–13867. [CrossRef]

55. Egambaram, O.P.; Kesavan Pillai, S.; Ray, S.S. Materials Science Challenges in Skin UV Protection: A Review. *Photochem. Photobiol.* **2020**, *96*, 779–797. [CrossRef] [PubMed]